Biocatalytic Self-Assembly on Magnetic Nanoparticles

Journal:	*ACS Applied Materials & Interfaces*
Manuscript ID	am-2017-15456e.R3
Manuscript Type:	Article
Date Submitted by the Author:	20-Dec-2017
Complete List of Authors:	Conte, Maria; University of Strathclyde, Pure and Applied Chemistry Sahoo, Jugal Kishore; University of Notre Dame, Department of Chemical and Biomolecular Engineering Abul-Haija, Yousef; University of Glasgow College of Science and Engineering, School of Chemistry Lau, King Hang Aaron; University of Strathclyde, Pure And Applied Chemistry Ulijn, Rein; Advanced Science Research Center (ASRC), City University New York

Biocatalytic Self-Assembly on Magnetic Nanoparticles

Maria P. Conte,[a] Jugal Kishore Sahoo,[a, b] Yousef M. Abul-Haija,[a, c] K. H. Aaron Lau,[a,] and Rein V. Ulijn[a, d, e, f, *]*

a. WestCHEM/Department of Pure & Applied Chemistry, University of Strathclyde, 99 George Street, Glasgow, G1 1RD, U.K.; E-mail: aaron.lau@strath.ac.uk

b. Department of Chemical and Biomolecular Engineering, McCourtney Hall, University of Notre Dame, IN, 46556

c. WestCHEM/School of Chemistry, The University of Glasgow, Glasgow G12 8QQ, UK

d. Advanced Science Research Center (ASRC) of the Graduate Center, City University of New York, 85 St Nicholas Terrace, New York NY10027, United States; E-mail: rein.ulijn@asrc.cuny.edu

e. Department of Chemistry and Biochemistry, City University of New York – Hunter College, 695 Park Ave., New York, NY 10065, USA.

f. PhD Program in Chemistry, The Graduate Center of the City University of New York, New York, NY 10016, USA.

KEYWORDS Peptides, Self-Assembly, Enzymes, Enzyme immobilization, Biocatalysis, Magnetic Nanoparticles

ABSTRACT Combining (bio-)catalysis and molecular self-assembly provides an effective approach for the production and processing of self-assembled materials, by exploiting catalysis to direct the assembly kinetics and hence control the formation of ordered nanostructures. Applications of (bio-)catalytic self-assembly in biologically interfacing systems and in nanofabrication have recently been reported. Inspired by self-assembly in biological cells, efforts to confine catalysts on flat or patterned surfaces to exert spatial control over molecular gelator generation and nanostructure self-assembly have also emerged. Building on our previous work in the area, we demonstrate in this report the use of enzymes immobilized onto magnetic nanoparticles (NPs) to spatially localize the initiation of peptide self-assembly into nanofibers around NPs. The concept is generalized for both an equilibrium biocatalytic system that forms stable hydrogels and a non-equilibrium system that normally has a preset lifetime. Characterization of the hydrogels shows that self-assembly occurs at the site of enzyme immobilization on the NPs, to give rise to gels with a "hub-and-spoke" morphology where the nanofibers are linked through the enzyme-NP conjugates. This NP-controlled arrangement of self-assembled nanofibers enables remarkable enhancements in the shear strength of both hydrogel systems, as well as a dramatic extension of the hydrogel stability in the non-equilibrium system. We are also able to show that the use of magnetic NPs enables external control of both the formation of the hydrogel and its overall structure by application of an external magnetic field. We anticipate that the enhanced properties and stimuli-responsiveness of our NP-enzyme system will have applications ranging from nanomaterial fabrication to biomaterials and biosensing.

1. Introduction

The combination of (bio)catalysis and supramolecular self-assembly[1-5] provides a powerful means to direct supramolecular materials formation.[6-11] This approach is inspired by dynamic materials found in biological systems, where self-assembly is often coupled to, and regulated by, catalysis.[12-14] A number of enzymes have been utilized in biocatalytic self-assembly, including phosphatases, esterases and proteases.[12, 14-15] These catalysts are typically dissolved in solutions of molecular precursors to enable catalytic formation of self-assembly gelator building blocks and consequent structure generation over time.

The possibility of employing surface immobilized catalysts has also been investigated, in order to achieve spatial control over the location of the self-assembly process. Williams *et al.* first employed immobilized thermolysin on an amine functionalized glass surface to enable localized self-assembly of Fmoc-protected peptides on a surface.[16] Vigier-Carriere *et al.* employed alkaline phosphatase immobilized in a polyelectrolyte multilayer to trigger the self-assembly and gelation of a Fmoc-protected tripeptide.[17] More recently, they employed chymotrypsin adsorbed on a surface to catalyze the condensation of short modified peptides into oligomers, which self-assemble into a fibrillar network at the interface.[18] In an example of non-enzymatic catalysts, Olive *et al.* employed patterned sulfonic acid groups to catalyze the local formation of supramolecular assemblies, leading to the formation of micropatterns of supramolecular structures.[13] In addition, the Xu

group has exploited localized biocatalytic assembly within living systems to influence the fate of cancer cells.[19-20]

It is clear that surface confined biocatalytic self-assembly holds promise both in biologically interfacing systems and as a tool in bottom-up nanofabrication.[16, 19-22] In fact, we recently highlighted the potential of selecting between gradually releasing and covalently immobilizing enzymes on a surface to obtain, respectively, a self-assembled bulk hydrogel and an ultrathin surface network of nanofibers.[23] However, to our knowledge, there are no reports that specifically demonstrate localized biocatalytic nucleation and self-assembly of nanostructures from nanoparticle-immobilized enzymes. Moreover, we are not aware of reports where the location of the immobilized enzymes could be externally controlled for nanostructure self-assembly.

In this study, we employed enzyme-magnetic nanoparticle (NP) conjugates for self-assembly initiation and post-assembly control of a hydrogel. To illustrate the general applicability of our immobilized enzyme NP approach, we selected two biocatalytic self-assembly systems that we have been studying: a thermodynamically controlled system based on thermolysin,[24] and a kinetic system based on chymotrypsin.[25] We followed the self-assembly process through a series of gelation experiments using reverse-phase high-performance liquid chromatography (RP-HPLC) measurements. We characterized the peptide nanostructures by transmission electron microscopy (TEM) and circular dichroism (CD) spectroscopy, and analyzed how the structural morphology influenced the mechanical strength of our gels, which was measured by oscillatory rheometry. Finally, we investigated the further consequences of the spatial organization of the catalytic

activity through manipulating the enzyme-NP conjugates with an externally applied magnetic field.

2. Results and Discussion

2.1. System Design and NP Preparation

System 1 is a thermodynamically controlled system that exploits thermolysin (from *Bacillus thermoproteolyticus*) for reversible enzymatic condensation of peptide precursors to form self-assembling gelators (Fig. 1b).[24] System 2 is a non-equilibrium, kinetically controlled system using chymotrypsin (from bovine pancreas) that has the potential to both generate self-assembly building blocks and break them down through competing acylation and hydrolysis reactions (Fig. 1b).[25]

Magnetic nanoparticles (NPs) were chosen to enable externally applied spatial control over the self-assembly process (*i.e.* stimuli-responsive behavior), without requiring chemical or direct mechanical manipulation of the NPs. We immobilized thermolysin and chymotrypsin on commercially available iron oxide NPs that have an average diameter of 500 nm (see section 1 in ESI and Fig. 1a). We found that the NP size chosen allowed for easy separation of the NPs with commercially available magnetic separation racks.

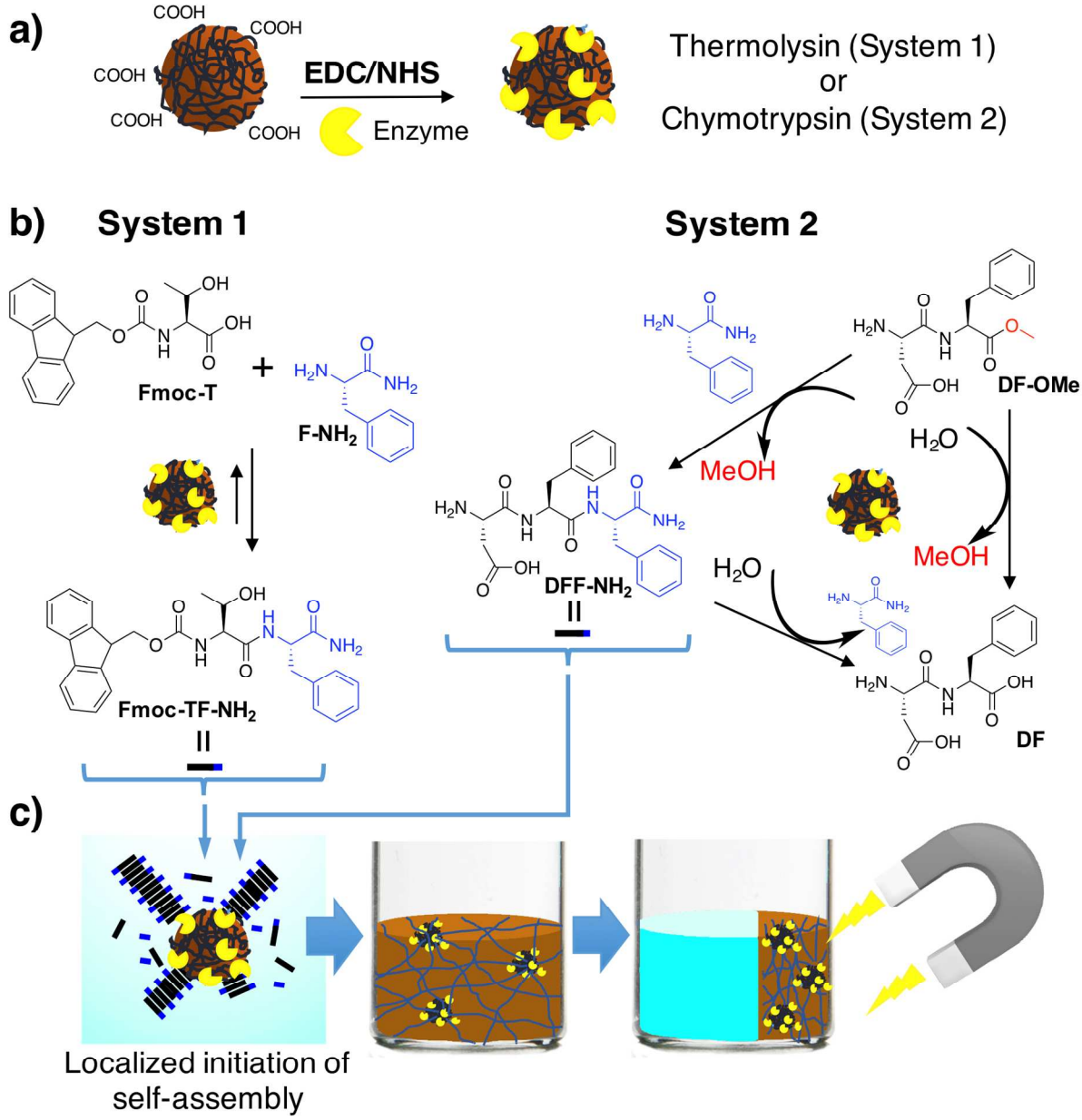

Figure 1: a) Schematic illustration of the enzyme immobilization by EDC/NHS coupling (see ESI). b) Reaction of the precursors with thermolysin-NP (System 1) and chymotrypsin-NPs (System 2) to give the self-assembly gelators. c) Schematics of the localized initiation of self-assembly onto the magnetic NPs and external manipulation of the formed hydrogel with a magnet.

Fluorescence spectroscopy was performed to monitor the activity of immobilized thermolysin and chymotrypsin *via* a previously reported and highly sensitive Förster resonance energy transfer (FRET) assay (see ESI section 2).[26] The NP-enzyme conjugates were washed multiple times to remove any weakly bound adsorbed enzymes. Significant activities arising from immobilized enzymes ("immobilized activities" in short) were measured on both thermolysin and chymotrypsin conjugates. Both NP systems gave activities equivalent to 5~10 μg/ml of "free" enzymes dissolved in solution (see ESI section 2).

2.2.Gelation Behavior of Thermolysin System 1

We have previously shown that thermolysin can catalyze amide bond formation between Fmoc-T and F-NH_2 to generate Fmoc-TF-NH_2 gelators, which then self-assemble into nanofibrous hydrogels (Fig. 1b).[24] In the present experiments, thermolysin-NP conjugates were added to a solution of the non-assembling precursors Fmoc-T (20 mM) and F-NH_2 (80 mM) in a glass vial and left to equilibrate. Samples of the mixture were taken at a series of time points for analysis by RP-HPLC to characterize the catalytic conversion.

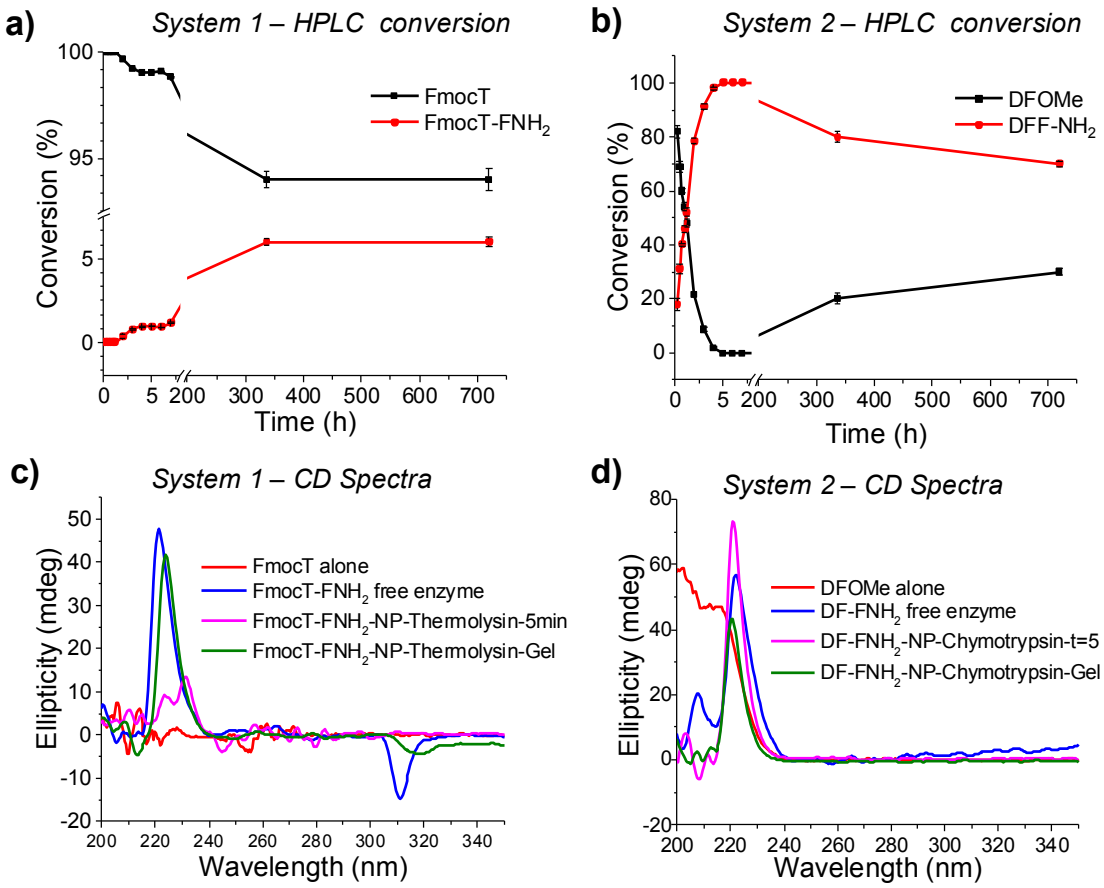

Figure 2: HPLC conversion of the precursors into gelators (a and b) and CD spectra of the peptide system (c and d) over the course of the experiments. HPLC retention times and protocols are described in ESI section 6. See the main text for CD peak assignments.

Fig. 2a shows that the conversion into Fmoc-TF-NH_2 slowly increased over time, reaching ca. 3.5% at 3 days and a plateau of 6% after 12 days. This low conversion was unexpected from preliminary visual inspection, which showed the formation of a light brown clear gel by the 4th day (Fig. 3a, inset). In comparison, our previous study with surface-released thermolysin shows a conversion of 30% and consequent gelation at the same time point.[23] Earlier studies using free enzymes show a conversion of ca. 35% after around 1h as a bulk gel is formed.[24]

Setting aside the ability to form a gel for the moment, the low conversion observed is reasonable considering the system conditions. First, the overall concentration of the enzyme is much lower compared to previous studies (~5 μg/ml vs. 1 mg/ml).[23-24] In addition, as shown previously,[23] surface-immobilized thermolysin catalyzes the conversion into gelators and the subsequent self-assembly only in the vicinity of the immobilization surface (likely facilitated by the low solubility of the Fmoc-peptides formed). We also observed that the NPs had gradually precipitated to the bottom of the vial over the multi-day experiment, which further lowered the effective enzyme concentration. Nonetheless, the fact that a bulk gel was formed in System 1 implies that the enzyme-NP conjugates were sufficiently dispersed throughout the bulk of the solution to enable nanofiber self-assembly without enzyme release from the NPs (see ESI).

The molecular organization of the self-assembled nanofibers in System 1 was first monitored with circular dichroism (CD) spectroscopy (Fig. 2c). The CD spectrum measured at the start of the experiment (CD measurement complete at t = 5 min) showed the appearance of a small positive peak around 220-230 nm. This peak grew in intensity upon gel formation, and it corresponds to the CD signature observed for gels formed with free enzymes, indicating the formation of chiral arrangements as previously reported, with the peak at 310 related to chirally organized fluorenyl groups.[27]

Secondly, TEM images of the gel material revealed a high density of nanofibers around the biocatalytic NPs (Fig. 3a and 3b). Apart from some micellar aggregates attributed to the presence of unreacted precursor Fmoc-T,[24] the images also show that the nanofibers emanating from the NPs were long and clearly defined, with a uniform diameter of ca. 15 nm similar to the free enzyme system.[24-25] This indicated that the self-assembly proceeded

from the NP surface in a process similar to regular free enzymatic catalysis. Furthermore, these nanofibers emanating from the enzyme-NP conjugates would have increased the masses and enlarged the sizes of the NPs, retarding NP diffusion. Also, as fiber growth proceeded, the enzymes on the NP surface would have become covered with nanofibers. Both these effects would slow the mass transport of precursors to the immobilized enzymes, thus resulting in the slowed and reduced conversion into Fmoc-TF-NH_2 observed in HPLC measurements.

2.3. Gelation Behavior of Chymotrypsin System 2

In the presence of free chymotrypsin, the precursors F-NH_2 and the dipeptide DF-OMe (*i.e.* aspartame) are known to form the tripeptide gelator DFF-NH_2, which self-assembles into a hydrogel composed of nanofibers (Fig. 1b). However, in a competing reaction, DFF-NH_2 is hydrolyzed also by chymotrypsin to give water soluble DF and F-NH_2. As a result of these competing processes, with the transacylation reaction proceeding at a faster rate than the hydrolysis, previous studies using free enzymes show that a gel is rapidly but transiently formed and the gel transitioned back to a sol in approximately 24 h under typical conditions.[25]

In the present study, an opaque dark brown gel was formed when we mixed the chymotrypsin-NP conjugates with the precursors DF-OMe (20 mM) and F-NH_2 (40 mM). This reaction proceeded within approximately 30 min, much quicker compared to the thermolysin System 1 but slower compared to the free chymotrypsin enzyme system where gelation occurs within minutes. HPLC analysis confirmed that the conversion into the tripeptide gelator DFF-NH_2 was complete within approximately 6 h (Fig. 2b and Fig. S5). The CD spectrum for System 2 shows a clear positive peak around 220 nm at t=5

min (Fig. 2d). This peak corresponds to the formation of chiral supramolecular arrangements as previously reported. [28]

In contrast to previous studies with free chymotrypsin, the hydrogel formed with the chymotrypsin-NP conjugate remained stable for several months until the end of our study. Only HPLC analysis of the gel material was able to discern a slow hydrolysis, with the percentage of conversion remaining as high as 80% after one month (Fig. 2b), much higher compared to that observed for the case of free chymotrypsin, where the percentage of conversion decreases to 10% after 72 h.[25] Thus, the lifetime of the hydrogel was dramatically enhanced by at least 30-fold, from 24 h to the end of HPLC studies at 1 month, simply by immobilizing the enzymes on the NPs.

TEM images of System 2, analogous to those of System 1, confirmed the formation of a network of nanofibers emanating from the surface of the NPs (Fig. 3c and d). This meant that the enzyme-NP conjugates were trapped by interlocked fibers emanating from the NPs and could not freely diffuse. As a consequence, the NP-immobilized enzymes would only be able to act on the tripeptide self-assembly building blocks diffusing to or in immediate contact with them. However, all the tripeptides would have already been assembled into the nanofibers (*i.e*. sequestered) except for a minority exchanging with the solution phase. Thus, the degradation of the self-assembled fibers was considerably retarded and the lifetime of the gel was significantly extended.

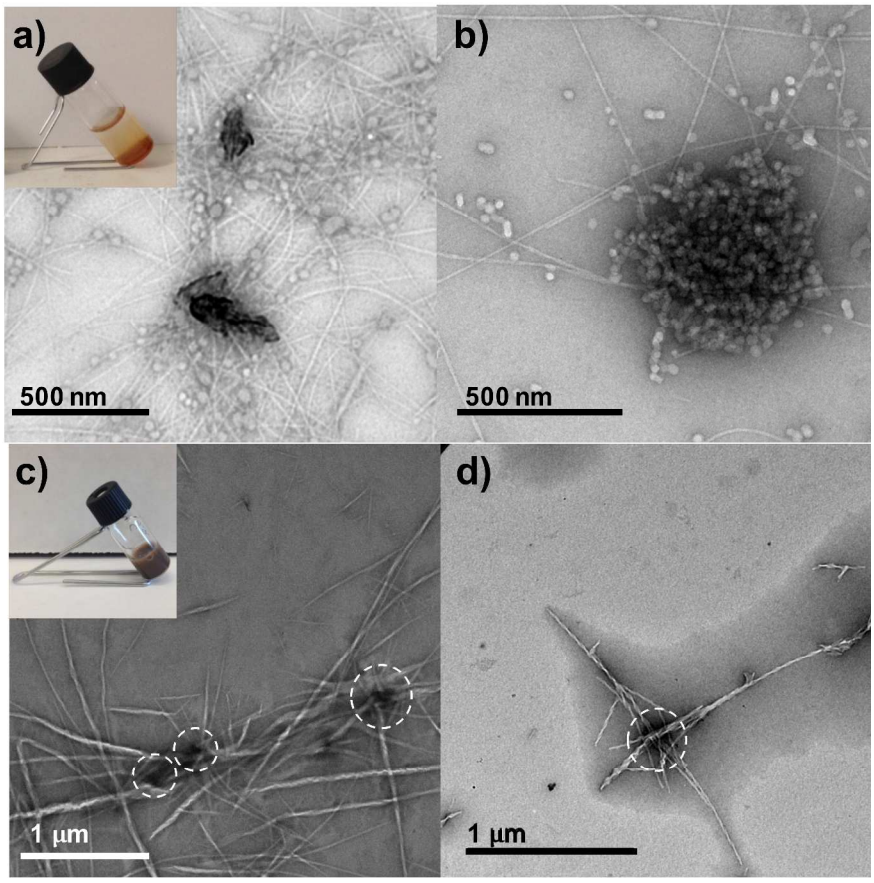

Figure 3: TEM images of the nanostructure formation catalyzed by the enzymes immobilized on the NPs for System 1 (a and b) and System 2 (c and d). The enzyme-NP conjugates are indicated by dashed circles for clarity. In the inset: images of the gels formed for System 1 (a) and System 2 (c).

2.4. Rheological Study of NP Connected Nanofibrous Hydrogel

As described in section 2.2, it is remarkable that the low precursor conversion observed in System 1 was still sufficient to form a bulk hydrogel. Moreover, TEM studies show nanofibrous networks connected by nanoparticle nodes (*i.e.* a hub-and-spoke morphology: Fig. 3) for both the thermolysin and chymotrypsin systems. A modification of nanostructural arrangement usually leads to a change in physical properties. Thus, we characterized the mechanical properties of the enzyme-NP catalyzed hydrogels using strain controlled frequency sweep rheometry (Fig. 4).

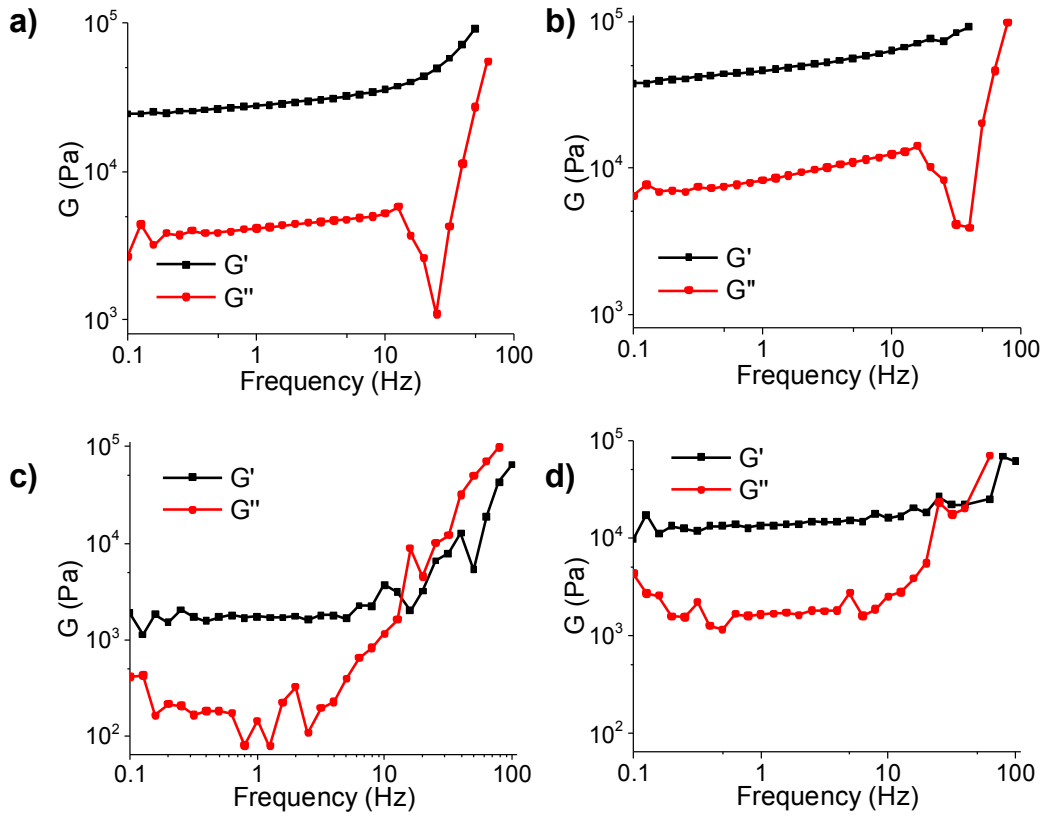

Figure 4: Dynamic frequency sweep experiments (0.06% maximum strain). a) FmocTF-NH_2 gels prepared with free thermolysin. G'= 35.5×10^3 Pa. b) Fmoc-TF-NH_2 gels prepared with thermolysin-NPs conjugate. G'= 51.5×10^3 Pa. c) DFF-NH_2 gels prepared with free chymotrypsin. G'= 1.89×10^3 Pa. d) DFF-NH_2 gels prepared with the chymotrypsin-NP conjugates. G'= 15.42×10^3 Pa. All G' values quoted refer to the average between 0.1 and 10 Hz.

For System 1, the use of the NP design resulted in a 44% increase of the storage modulus G', from 36×10^3 Pa for the gel formed with free thermolysin, to 52×10^3 Pa for the gel formed with the enzyme-NP conjugates (values referring to the average in the range between 0.1 and 10 Hz). However, even this modest increase in G' (and actually also in G'') is surprising because the conversion of the precursors to the self-assembling gelators was much lower in the NP system (6% vs. 81%[24]). This suggests that the NP-

nanofiber hub-and-spoke morphology greatly enhanced the mechanical properties of a self-assembled hydrogel.

The effect of incorporating the NPs is more dramatically evident in System 2, where G' increased by almost one order of magnitude, from 1.9×10^3 Pa for the gel obtained with free chymotrypsin to 15×10^3 Pa for the gel obtained with the enzyme-NP conjugates. Unlike System 1, high conversion of the precursors was obtained in System 2 using both the NP-mediated and free enzyme processes. We can therefore attribute the large increase in shear stiffness to the immobilization of the enzyme on the NPs and the resulting nanofiber arrangement around the NPs.

Saiani *et al.* likewise observed that the mechanical properties of a self-assembled gel can be improved with a heterogeneous distribution of nanofibers.[29] In their study, macroscopic increases in gelator concentrations were correlated with increases in the microscale heterogeneity of the nanofiber distribution. Although Saiani *el al.,* did not study the mechanisms of nanofiber initiation and aggregation in detail, their results do suggest that higher enzyme concentrations, which give higher rates of self-assembly, may promote localized distributions of nanofibers. In our system, the large number of enzymes that can be immobilized on each NP acts to increase the local concentration of gelators formed. Moreover, the slow diffusion of NPs (relative to dissolved enzymes) reduces the spatial distribution of gelators formed. Therefore, using our NP approach, localization of self-assembly and enhancement in properties may be enabled for a wide range of enzyme kinetics, as illustrated by Systems 1 and 2.

2.5. External Manipulation of Hydrogel System

The magnetic nature of our enzyme-NP conjugates offered a convenient way to manipulate our self-assembly system. Given the long time required for System 1 to gel, we focused on the chymotrypsin System 2. In a first set of experiments to test the basic response to an externally applied magnetic field, 100 μl of the mixture of precursors and chymotrypsin-NP conjugates was placed within a 96-well cell culture plate, and a small permanent magnet was introduced, immediately after mixing the components. We tested the magnet placement in three different positions (Fig. S6): on top of the well (Position 1), and 1.2 cm and 2.4 cm from the side of the well (Positions 2 and 3, respectively). The system was then left to equilibrate.

When the magnet was placed in Position 1, the NPs immediately migrated to the top of the solution, "switching off" the gelation process (Fig. S6a). When the magnet was placed in Position 2, formation of a gel with a gradation of color was observed overnight (Fig. S6b). When the magnet was in position 3, no effect on the gel appearance was observed (Fig. S6c), but the gelation occurred slower compared to the case when no magnet was introduced (~4 h compared to 30 min), suggesting that the NPs were displaced by the magnet to some extent.

The color gradation of the gel could actually indicate a gradient in the density of self-assembled nanofibers across the gel, resulting from the slow migration of the NPs towards the magnet. Such a variation in nanofiber density could presumably correspond to a gradient in mechanical properties. However, local mechanical characterization of a soft hydrogel is challenging and awaits further study.

In a second experiment, to investigate the effect of a magnetic field after the gel has formed, the magnet was placed next to a vial containing an already formed gel (Fig. 5). This gel was observed to slowly shrink over time, approximately by 50% after 1 weak, and finally reaching approximately 15% of its original volume after one month. The change in the gel volume after 1 month was permanent (removal of the magnet does not restore gel volume). HPLC analysis showed a much lower concentration of DFF-NH_2 in the transparent supernatant outside the gel (conversion of less than 20%) than in the contracted gel part of the system (conversion remaining as high as 70% after 1 month; see section 9 in ESI). This difference in DFF-NH_2 content is consistent with the TEM characterization that shows very few fibers in the supernatant, but a high density of fibers in the contracted gel (Fig. 5).

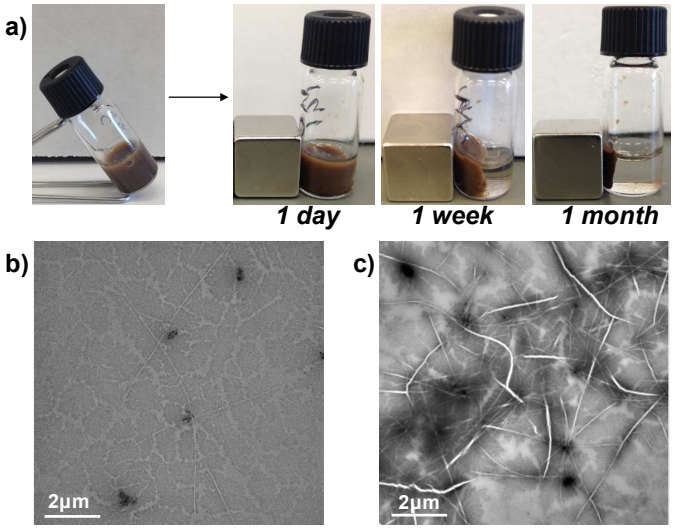

Figure 5: (a) Images showing the effect of a magnetic field on the DF-FNH_2 gel formed with the chymotrypsin-NPs. The gel shrank to ~15% of its initial volume after 1 month. TEM images of transparent supernatant collected upon separation with the magnetic cube (b) and of the compacted gel (c).

This second experiment shows that the gel may be separated together with the NP conjugates, even when the strength of the nanofibrous network and the osmotic pressure associated with "squeezing out" the supernatant are acting against the NPs. This implies that the self-assembled nanofibers were strongly associated with the NP surface (as also suggested by the significant enhancement of mechanical properties for the NP-mediated hydrogels: Fig. 4). This integration was possible even though the gels were formed from a relatively low precursor conversion (Fig. 2), which underscores the importance of the nanofiber hub-spoke organization.

In fact, a strong association of the nanofibers with the NPs as well as the relatively slow precursor conversion kinetics observed (see sections 2.2 and 2.3) are both expected, if gelator production and nanofiber self-assembly were localized on the enzyme-NP surfaces such that nanofibers could be concentrated and adhered around the NPs. This was indeed observed in TEM (Fig. 3). The possibility to closely specify the location of self-assembly was also suggested by our previous observation of nanofiber networks on enzyme-functionalized flat surfaces.[23] Thus the overall experimental evidence supports the hypothesis that surface-immobilized enzymes could direct nucleation and self-assembly of nanostructures.

3. Conclusion

We demonstrated the use of enzymes immobilized on magnetic NPs for both an equilibrium and a non-equilibrium biocatalytic self-assembling peptide hydrogel system. By simply immobilizing the biocatalyst on NPs and hence localizing the initiation of nanofiber self-assembly, we could change the hydrogel nanostructural organization from

a random arrangement to an overall "hub-and-spoke" morphology where the nanofibers can be linked through the enzyme-NP conjugates. This resulted in up to a ~10-fold increase of the mechanical modulus of the hydrogel compared to a conventional soluble enzyme system. We hypothesize that the nodes of concentrated nanofibers enhance the mechanical integrity of the fibrous network. Localization of the enzyme also dramatically restricted the enzyme's ability to mediate degradation side reactions that would otherwise have dissipated the nanofibers in a non-equilibrium system, and thus enabled unprecedented control (a >30-fold extension) in the lifetime of a self-assembled hydrogel.

In addition, we demonstrated magnetic manipulation of the self-assembly system. Application of an external magnetic field enabled "switching off" of self-assembly. Application post-gelation could pull the NPs along with their associated nanofibers, resulting in a more than 6-fold compaction in the hydrogel volume. If functional groups were incorporated into the nanofibers, behaviors that depend on chemical concentrations may also be enabled. The expulsion of the sol phase is also essentially a mechanism for material release.

In summary, by immobilizing the (bio)catalyst on magnetic NPs and hence localizing the nucleation of (bio)catalytic nanofiber self-assembly, it is possible not only to enhance the mechanical properties of a nanofibrous hydrogel network, but also to control the timing of its formation, its lifetime, as well as to confer stimuli-responsiveness to the self-assembled nanostructure.

ASSOCIATED CONTENT

Supporting Information: Details on experimental procedures and sample characterization.

AUTHOR INFORMATION

Corresponding Author

*E-mail: aaron.lau@strath.ac.uk

*E-mail: rein.ulijn@asrc.cuny.edu

Author Contributions

The manuscript was written through contributions of all authors. All authors have given approval to the final version of the manuscript.

ACKNOWLEDGMENT

The authors gratefully acknowledge the financial support by the EC 7th Framework Programme Marie Curie Actions via the European ITN SMARTNET No. 316656. This material is based upon work supported by, or in part by, the U. S. Army Research Laboratory and the U. S. Army Research office under contract/grant number W911NF-16-1-0113. They also acknowledge Margaret Mullin from University of Glasgow and Tong Wang from the ARSC in CUNY for their help in TEM imaging.

REFERENCES

1. Hartgerink, J. D.; Beniash, E.; Stupp, S. I., Self-Assembly and Mineralization of Peptide-Amphiphile Nanofibers. *Science* **2001,** *294* (5547), 1684-1688.

2. Whitesides, G. M.; Grzybowski, B., Self-Assembly at All Scales. *Science* **2002,** *295* (5564), 2418-2421.

3. Lehn, J.-M., Toward Self-Organization and Complex Matter. *Science* **2002,** *295* (5564), 2400-2403.

4. Mattia, E.; Otto, S., Supramolecular Systems Chemistry. *Nat. Nano.* **2015,** *10* (2), 111-119.

5. Yang, Z.; Liang, G.; Xu, B., Enzymatic Hydrogelation of Small Molecules. *Acc. Chem. Res.* **2008,** *41* (2), 315-326.

6. Cui, H.; Webber, M. J.; Stupp, S. I., Self-Assembly of Peptide Amphiphiles: From Molecules to Nanostructures to Biomaterials. *J. Pept. Sci.* **2010,** *94* (1), 1-18.

7. Liu, Y.; Terrell, J. L.; Tsao, C.-Y.; Wu, H.-C.; Javvaji, V.; Kim, E.; Cheng, Y.; Wang, Y.; Ulijn, R. V.; Raghavan, S. R.; Rubloff, G. W.; Bentley, W. E.; Payne, G. F., Biofabricating Multifunctional Soft Matter with Enzymes and Stimuli-Responsive Materials. *Adv. Funct. Mater.* **2012,** *22* (14), 3004-3012.

8. Fichman, G.; Gazit, E., Self-Assembly of Short Peptides to Form Hydrogels: Design of Building Blocks, Physical Properties and Technological Applications. *Acta Biomater.* **2014,** *10* (4), 1671-1682.

9. Webber, M. J.; Appel, E. A.; Meijer, E. W.; Langer, R., Supramolecular Biomaterials. *Nat. Mater.* **2016,** *15* (1), 13-26.

10. Zhou, J.; Li, J.; Du, X.; Xu, B., Supramolecular Biofunctional Materials. *Biomaterials* **2017,** *129*, 1-27.

11. Hirst, A. R.; Escuder, B.; Miravet, J. F.; Smith, D. K., High-Tech Applications of Self-Assembling Supramolecular Nanostructured Gel-Phase Materials: From Regenerative Medicine to Electronic Devices. *Angew. Chem. Int. Ed.* **2008,** *47* (42), 8002-8018.

12. Hirst, A. R.; Roy, S.; Arora, M.; Das, A. K.; Hodson, N.; Murray, P.; Marshall, S.; Javid, N.; Sefcik, J.; Boekhoven, J.; van Esch, J. H.; Santabarbara, S.; Hunt, N. T.; Ulijn, R. V., Biocatalytic Induction of Supramolecular Order. *Nat. Chem.* **2010,** *2* (12), 1089-1094.

13. Olive, A. G. L.; Abdullah, N. H.; Ziemecka, I.; Mendes, E.; Eelkema, R.; van Esch, J. H., Spatial and Directional Control over Self-Assembly Using Catalytic Micropatterned Surfaces. *Angew. Chem. Int. Ed.* **2014,** *126* (16), 4216-4220.

14. Yang, Z.; Gu, H.; Fu, D.; Gao, P.; Lam, J. K.; Xu, B., Enzymatic Formation of Supramolecular Hydrogels. *Adv. Mater.* **2004,** *16* (16), 1440-1444.

15. Debnath, S.; Roy, S.; Ulijn, R. V., Peptide Nanofibers with Dynamic Instability through Nonequilibrium Biocatalytic Assembly. *J. Am. Chem. Soc.* **2013,** *135* (45), 16789-16792.

16. Williams, R. J.; Smith, A. M.; Collins, R.; Hodson, N.; Das, A. K.; Ulijn, R. V., Enzyme-Assisted Self-Assembly under Thermodynamic Control. *Nat. Nanotechnol.* **2009,** *4* (1), 19-24.

17. Vigier-Carrière, C.; Garnier, T.; Wagner, D.; Lavalle, P.; Rabineau, M.; Hemmerlé, J.; Senger, B.; Schaaf, P.; Boulmedais, F.; Jierry, L., Bioactive Seed Layer for Surface-Confined Self-Assembly of Peptides. *Angew. Chem. Int. Ed.* **2015,** *54* (35), 10198-10201.

18. Vigier-Carrière, C.; Wagner, D.; Chaumont, A.; Durr, B.; Lupattelli, P.; Lambour, C.; Schmutz, M.; Hemmerlé, J.; Senger, B.; Schaaf, P.; Boulmedais, F.; Jierry, L., Control of Surface-Localized, Enzyme-Assisted Self-Assembly of Peptides through Catalyzed Oligomerization. *Langmuir* **2017,** *33* (33), 8267-8276.

19. Yang, Z. M.; Xu, K. M.; Guo, Z. F.; Guo, Z. H.; Xu, B., Intracellular Enzymatic Formation of Nanofibers Results in Hydrogelation and Regulated Cell Death. *Adv. Mater.* **2007,** *19* (20), 3152-3156.

20. Kuang, Y.; Shi, J.; Li, J.; Yuan, D.; Alberti, K. A.; Xu, Q.; Xu, B., Pericellular Hydrogel/Nanonets Inhibit Cancer Cells. *Angew. Chem. Int. Ed.* **2014,** *53* (31), 8104-8107.

21. Pires, R. A.; Abul-Haija, Y. M.; Costa, D. S.; Novoa-Carballal, R.; Reis, R. L.; Ulijn, R. V.; Pashkuleva, I., Controlling Cancer Cell Fate Using Localized Biocatalytic Self-Assembly of an Aromatic Carbohydrate Amphiphile. *J. Am. Chem. Soc.* **2015,** *137* (2), 576-579.

22. Fabijanic, K. I.; Perez-Castillejos, R.; Matsui, H., Direct Enzyme Patterning with Microcontact Printing and the Growth of Zno Nanoparticles on the Catalytic Templates at Room Temperature. *J. Mater. Chem.* **2011,** *21* (42), 16877-16879.

23. Conte, M. P.; Lau, K. H. A.; Ulijn, R. V., Biocatalytic Self-Assembly Using Reversible and Irreversible Enzyme Immobilization. *ACS Appl. Mater. Interfaces* **2017,** *9* (4), 3266-3271.

24. Sasselli, I. R.; Pappas, C. G.; Matthews, E.; Wang, T.; Hunt, N. T.; Ulijn, R. V.; Tuttle, T., Using Experimental and Computational Energy Equilibration to Understand Hierarchical Self-Assembly of Fmoc-Dipeptide Amphiphiles. *Soft Matter* **2016**, *12*, 8307-8315

25. Pappas, C. G.; Sasselli, I. R.; Ulijn, R. V., Biocatalytic Pathway Selection in Transient Tripeptide Nanostructures. *Angew. Chem. Int. Ed.* **2015,** *54* (28), 8119-8123.

26. Beljonne, D.; Curutchet, C.; Scholes, G. D.; Silbey, R. J., Beyond Förster Resonance Energy Transfer in Biological and Nanoscale Systems. *J. Phys. Chem. B* **2009,** *113* (19), 6583-6599.

27. Cheng, G.; Castelletto, V.; Moulton, C. M.; Newby, G. E.; Hamley, I. W., Hydrogelation and Self-Assembly of Fmoc-Tripeptides: Unexpected Influence of Sequence on Self-Assembled Fibril Structure, and Hydrogel Modulus and Anisotropy. *Langmuir* **2010,** *26* (7), 4990-4998.

28. Marchesan, S.; Waddington, L.; Easton, C. D.; Winkler, D. A.; Goodall, L.; Forsythe, J.; Hartley, P. G., Unzipping the Role of Chirality in Nanoscale Self-Assembly of Tripeptide Hydrogels. *Nanoscale* **2012,** *4* (21), 6752-6760.

29. Guilbaud, J.-B.; Rochas, C.; Miller, A. F.; Saiani, A., Effect of Enzyme Concentration of the Morphology and Properties of Enzymatically Triggered Peptide Hydrogels. *Biomacromolecules* **2013,** *14* (5), 1403-1411.

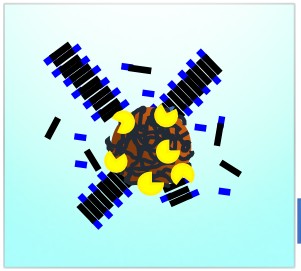

Localized initiation of self-assembly

Nanostructural organization

Stimuli responsive manipulation

Unique functional properties